Sigma J Eng Nat Sci, Vol. 42, No. 5, pp. 1367–1377, October, 2024

Sigma Journal of Engineering and Natural Sciences
Web page info: https://sigma.yildiz.edu.tr
DOI: 10.14744/sigma.2024.00106

Research Article

Robust power stabilizing control of a grid-connected inverter using linear matrix inequality

Panha SOTH[1,2], Sokleng NOUN[3], Heng TANG[1], Chanmoly OR[4], Sarot SRANG[5], Yahya DANAYIYEN[6], Chivon CHOEUNG[1,*]

[1]*Faculty of Electricity, National Polytechnic Institute of Cambodia, Phnom Penh, 120407 Cambodia*
[2]*Graduate School, National Polytechnic Institute of Cambodia, Phnom Penh, 120407 Cambodia*
[3]*Technique and Planning Division, Electricity of Cambodia, Siem Reap, 120407, Cambodia*
[4]*Research and Innovation Center, Institute of Technology of Cambodia, Phnom Penh, 120407, Cambodia*
[5]*Department of Industrial and Mechanical Engineering, Institute of Technology of Cambodia, Phnom Penh, 120407, Cambodia*
[6]*Department of Electrical and Electronics Engineering, Karadeniz Technical University, Trabzon, 61080, Türkiye*

ARTICLE INFO

Article history
Received: 15 May 2023
Revised: 18 August 2023
Accepted: 11 October 2023

Keywords:
Grid-Connected Inverter; Linear Matrix Inequality (LMI); Robust Power Control

ABSTRACT

A linear matrix inequality (LMI)-based robust stabilizing control is proposed in this paper for a three-phase grid-connected inverter (GCI) with L-filtered output. Previous research, such as MPC, required high computational power and precise modeling in order to obtain offset-free performance. Achieving optimal performance in the case of PI control poses a persistent challenge in terms of gain tuning. This proposed control strategy effectively addresses the aforementioned issues by the utilization of systematic control design, incorporating integral action to mitigate the presence of offset error. The set of state feedback and integral gain is obtained by solving the LMI-based optimization problem to maximize the convergence rate to a steady state in the presence of uncertainty in the L-filter. The mentioned uncertainties are represented by potential ranges of the inductor values. Output power delivery can be simply regulated by a computed reference state using a given power reference and measured grid current and voltage. The effectiveness of the proposed method is verified through simulations. The proposed robust control method demonstrates a significant decrease in ripple, with a reduction of 86.66% when compared to the conventional PI control approach.

Cite this article as: Soth P, Noun S, Tang H, Or C, Srang S, Danayiyen Y, Choeung C. Robust power stabilizing control of a grid-connected inverter using linear matrix inequality. Sigma J Eng Nat Sci 2024;42(5):1367–1377.

***Corresponding author.**
*E-mail address: choeungchivon@npic.edu.kh

This paper was recommended for publication in revised form by Regional Editor Ahmet Selim Dalkilic

Published by Yıldız Technical University Press, İstanbul, Turkey

INTRODUCTION

The demand for electricity has experienced a significant surge in recent decades, mostly driven by the emergence of electric vehicles and the process of urbanization. Renewable energies (REs) such as solar photovoltaic, winds turbine, and energy storage systems (ESS) are increasingly being integrated into the distribution system, and distribution generation (DG) to provide and fulfill various benefits such as a dependable, secure, and highly efficient energy supply to the loads. In DG, electrical machines [1–3] play a crucial role in various applications such as power generation, distribution, and industrial processes. They are designed to efficiently convert, transmit, and control electrical power within a network, allowing for the seamless distribution of energy across multiple locations. It is worth noting that the short circuit ratio (SCR) holds significant effect over the maximum power transfer capacity of the grid-connected inverter. The SCR is a metric used to quantify the robustness of the grid. It is determined by calculating the ratio between the short circuit power at the point of common coupling (PCC) and the rated power of the inverter [4]. When the short-circuit ratio (SCR) falls below the range of 6-10, it indicates a state of grid weakness. When the SCR exceeds a value of 20, it indicates a high level of strength in the grid [5]. Based on the established definition of the SCR, it can be inferred that an augmentation in the rated power of the inverter or the impedance of transmission will result in a decrease in the SCR, thereby rendering the grid less robust. The voltage at the PCC exhibits significant variability when a substantial quantity of active power is fed into a grid with low strength. Therefore, for it to maintain the voltage at the PCC within its specified rating [6], it is necessary to employ reactive power regulation. The power transfer capability of a grid-connected inverter is limited by the inverse relationship between output reactive power and output active power, given that the total rated power of the inverter remains constant. Because the power quality (PQ) issue poses significant technological problems for REs attempting to integrate with DG, grid connection is largely dependent on the grid connected inverter (GCI)'s control technology. Consequently, in utility applications, a GCI is at the heart of the interfacing devices between REs and the grid. Moreover, many modern and efficient control strategies have been proposed for GCI to provide a well-regulated power output and stability to the system.

Predictive controls have been studied in [7–14] for three-phase GCIs. In [7], a model-free predictive control is proposed by deriving the mixed sensitivity H∞ controller from input/output measurements to reach optimal predictive performance. Model Predictive Control (MPC) has been carried out for three-phase GCIs with L-filter [8,9] and LCL-filter [10,11]. To cancel out the sensitivity of the grid disturbance, a disturbance observer (DOB)-based on an extended Kalman filter has been employed in [8] with a dichotomy algorithm. A direct power control-based predictive control has been studied in [9] to provide a rapid dynamic response for a three-phase GCI. The switching time of this converter is obtained by minimizing the square errors of the active and reactive power. Both the dynamic and steady-state performance of this predictive direct power control is worthwhile. A generalized predictive control, a subtype of continuous control set-model predictive control (CCS-MPC), is suggested in [10] as a means of reducing computing complexity. Linear matrix inequality (LMI)-based MPC with DOB has been studied in [11] to provide robustness to the GCI system. The weighting matrix of the MPC cost function and the DOB gain are determined by solving LMI-based optimization problems with consideration of the uncertainty model. An FCS-MPC is proposed in [12] for a three-phase four-leg GCI. This method is an easily realized control method with good dynamic performance and robustness. Predictive-based deadbeat control is proposed in [13] and [14] with a combination of Luenberger observers to estimate the future value of the grid current. This method provides a high-speed response from the nature of deadbeat control, but the determining of the observer gain is not optimal. To summarize, the predictive control provides a fast dynamic response and with the help of DOB, the offset error can be removed. Although conventional MPC is effective in controlling systems with disturbances, noise, and uncertainty, it demands a considerable amount of computational power leading to a high sampling frequency. In addition, the system may experience steady-state errors if the effect of disturbances and uncertainties is not considered, which is why the use of DOB is crucial.

Classical PI control is one of the most well-known controllers and has been proposed in [15–18] for three-phase GCIs. In the presence of unidentified grid parameters, a phase-locked loop (PLL)-free technique has been investigated in [16]. Through a Lyapunov stability analysis, the controller and observer of the design of this technique are motivated and validated. Simply, grid voltage feedback and phase angle are not necessary for this current control; only the current feedback is needed. A PI-based controller for three-phase GCI is suggested in [17] and is capable of handling a varying grid. The proposed controller in [17] employs two parallel current control loops, one for positive and another for negative sequence current signals, to maintain constant current or non-oscillating active and reactive power in three-phase grid-connected inverters (GCIs). However, achieving optimal performance using this method requires multi-loop gain tuning, which is a disadvantage. To address this issue, an adaptive PID control technique with disturbance observer (DOB) for LCL-filtered GCIs is proposed in [18]. The DOB ensures that the steady-state performance of the system remains largely unaffected by uncertainties. Although the adaptive learning

rule employed in this method is complex and relatively slow, it is essential for improving robustness and performance. In conclusion, while the PI control approach is generally acceptable, achieving optimal performance with it remains a challenge due to the difficulties involved in gain tuning. The proposed adaptive PID control approach with DOB offers a potential solution to this problem but at the cost of increased complexity and slower response times. A state feedback control has been studied with a combination of integral control and DOB in the dq-rotational frame [19]. This method proposed a systematic controller design for GCI with LCL-filter using pole placement to determine controller stabilizing gain.

The LMI-based control method has been the subject of extensive research and application in power converters, such as three-phase inverters [20–25], single-phase inverters [26], three-phase AC-DC converters [27,28], and grid-connected inverters [29,30], due to its systematic design and optimization capabilities.. An LMI-based control is proposed for a three-phase inverter capable of working in islanded and grid-connected modes. In addition, two feedback controls are designed for each operation mode with the inclusion of uncertainty of grid impedance. An improvement is discussed in [21] by adding one step ahead prediction to eliminate the time delay using robust state predictor and Kalman filter. To provide an inverter that can withstand the unbalanced and nonlinear load conditions, [22] has been studied to regulate the output voltage supplying a three-phase balanced sinusoidal waveform using the resonant controller. Another approach, [23] proposed an LMI-based continuous control set model predictive control (CCS-MPC) to regulate the output voltage with help from LMI based robust disturbance observer. This method provides a good output tracking performance with improved transient response during the load change. Instead of using LMI based method for the observer design, [24] employed the Kalman filter so that the offset-free output voltage can be obtained. In [25], a robust interpolation method is designed for a three-phase LC-filtered inverter. The gain of this method is determined by an interpolation between tight and loose gain to get the best benefits of both types of gains. An LMI-based approach was also proposed for a single-phase droop-controlled inverter [26]. This scheme utilizes static output feedback with consideration of parameter variation for controller design. In the case of three-phase DC-AC converter, a cascaded controller is proposed in [27] for a fast-charging capability using the CC-CV charging stage. To ensure stability without any offset error, the inner loop of the controller employed state feedback integral control based on LMI. Afterward, the output charging voltage and current are controlled by an outer loop PI controller. In addition to LMI-based control, a linear quadratic regulator-based suboptimal control has been studied for an interlink converter for a hybrid AC-DC microgrid [28]. As a result, this converter is able to manage the power demand balance under numerous unknown filter parameters with superior output performances compared to those of PI. In [29], another systematic control design has been discussed for grid-connected converters using LMI-based optimal state feedback control. Despite not considering the uncertainty model, this strategy also guarantees overall stability with a response that has zero offset error. It has also been improved by [30] to work under unbalanced grid conditions by eliminating the negative sequence current using dual current control.

Based on the literature review mentioned above, here, we proposed a state feedback integral controller to provide closed-loop stability in a three-phase grid-connected inverter (GCI) without steady-state error. The proposed GCI system can provide instantaneous power from a DC source to the grid with ease and superior reference tracking thanks to integral control. This study enhances [29] by using an uncertainty model to offer a wider range of stability even with unreliable filter parameters. Additionally, by using reference state calculation, this method offers a greater capability for controlling the power flow to the AC grid as opposed to simply regulating the grid current. Furthermore, an optimization problem is included in this paper to minimize the settling time so that the set of stabilizing gains is computed using MATLAB. By laying out a systematic control design, the effort of gain tuning is lesser compared to PI control. To verify the effectiveness of the proposed control method, a comparison between conventional PI power control is conducted in simulation studies. This article is structured into distinct sections, namely: an introduction, a discussion on continuous and discrete time models, an exploration of reference state computation, an analysis of simulation studies, and a concluding section. The introductory section of this study provides a concise overview of the issues, previous studies, and the proposed research approach. The second half of this paper presents the description of the inverter model in both continuous and discrete times, namely in the dq-frame. The subsequent section of this paper will dive into the discussion of the present reference realization, employing a straightforward instantaneous power relationship within the dq-frame. Subsequently, the outcomes of the aforementioned control strategy are validated by PSIM simulation and juxtaposed with the outcomes of conventional PI control. Eventually, the article concludes with a succinct conclusion in its final part.

CONTINUOUS AND DISCRETE TIME MODELS

In this section, an easily understood process of a three-phase grid-connected inverter with *L*-filters is discussed. The topology of the GCI is shown in Figure 1.

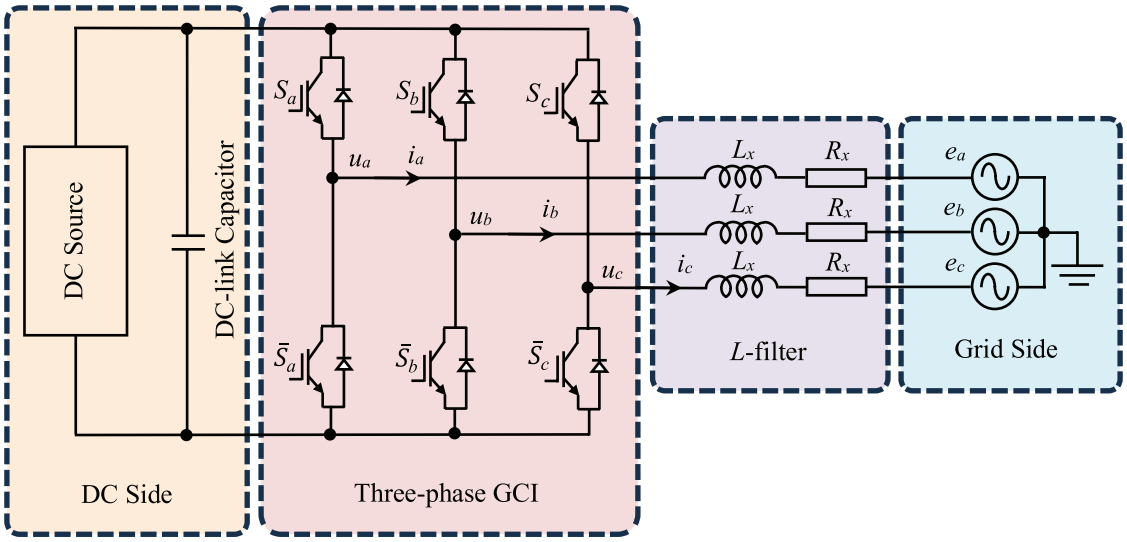

Figure 1. Three-phase grid-connected inverter with L-filter.

By applying Kirchhoff's law to the GCI, the system dynamic can be obtained in *abc*-frame as follows:

$$\begin{cases} L_x \dfrac{di_a(t)}{dt} = u_a(t) - R_x i_a(t) - e_a(t) \\ L_x \dfrac{di_b(t)}{dt} = u_b(t) - R_x i_b(t) - e_b(t) \\ L_x \dfrac{di_c(t)}{dt} = u_c(t) - R_x i_c(t) - e_c(t) \end{cases} \tag{1}$$

where L_x, R_x, $\mathbf{e}_{abc} = \begin{bmatrix} e_a & e_b & e_c \end{bmatrix}^T$, and $\mathbf{i}_{abc} \begin{bmatrix} i_a & i_b & i_c \end{bmatrix}^T$ are filter inductance, resistance, grid voltage vector, and grid current vector, respectively. The pole voltage $\mathbf{u}_{abc} = \begin{bmatrix} u_a & u_b & u_c \end{bmatrix}^T$. The dynamic (1) can be transformed to *dq*-synchronous frame as:

$$\begin{cases} \dfrac{di_d(t)}{dt} = -\dfrac{R_x}{L_x} i_d(t) - \omega i_q(t) + \dfrac{1}{L_x} u_d(t) - \dfrac{1}{L_x} e_d(t) \\ \dfrac{di_q(t)}{dt} = -\dfrac{R_x}{L_x} i_q(t) + \omega i_d(t) + \dfrac{1}{L_x} u_q(t) - \dfrac{1}{L_x} e_q(t) \end{cases}. \tag{2}$$

The relationship between *abc*-frame and *dq*-frame can be validated as follows:

$$\mathbf{i}_{dq}(t) = \frac{2}{3}\mathbf{T}(t)\mathbf{i}_{abc}(t),\ \mathbf{i}_{abc}(t) = \frac{3}{2}\mathbf{T}^T(t)\mathbf{i}_{dq}(t) \tag{3}$$

$$\mathbf{e}_{dq}(t) = \frac{2}{3}\mathbf{T}(t)\mathbf{e}_{abc}(t),\ \mathbf{e}_{abc}(t) = \frac{3}{2}\mathbf{T}^T(t)\mathbf{e}_{dq}(t) \tag{4}$$

where ω is the angular frequency of the grid which can be obtained by the phase-locked loop,

$$\mathbf{T}(t) = \begin{bmatrix} \cos(\omega t) & \cos(\omega t - 2\pi/3) & \cos(\omega t + 2\pi/3) \\ \sin(\omega t) & \sin(\omega t - 2\pi/3) & \sin(\omega t + 2\pi/3) \end{bmatrix}. \tag{5}$$

The dynamic (2) can be expressed as a vector form as bellow:

$$\begin{cases} \dfrac{d\mathbf{x}(t)}{dt} = \mathbf{A}_c\mathbf{x}(t) + \mathbf{B}_c\mathbf{u}(t) + \mathbf{D}_c\mathbf{e}(t) \\ \mathbf{y}(t) = \mathbf{C}\mathbf{x}(t) \end{cases} \tag{6}$$

where $\mathbf{C}$ is output matrix $\mathbf{C} = \begin{bmatrix} 1 & 0 \\ 0 & 1 \end{bmatrix}$, $\dfrac{d\mathbf{x}(t)}{dt} = \begin{bmatrix} \dfrac{di_d(t)}{dt} \\ \dfrac{di_q(t)}{dt} \end{bmatrix}$,

$$\mathbf{A}_c = \begin{bmatrix} -\dfrac{R_x}{L_x} & -\omega \\ \omega & -\dfrac{R_x}{L_x} \end{bmatrix}, \mathbf{x}(t) = \begin{bmatrix} i_d(t) \\ i_q(t) \end{bmatrix},$$

$$\mathbf{B}_c = \begin{bmatrix} \dfrac{1}{L_x} & 0 \\ 0 & \dfrac{1}{L_x} \end{bmatrix},\ \mathbf{u}(t) = \begin{bmatrix} u_d(t) \\ u_q(t) \end{bmatrix},\ \mathbf{D}_c = \begin{bmatrix} -\dfrac{1}{L_x} & 0 \\ 0 & -\dfrac{1}{L_x} \end{bmatrix},$$

$$\mathbf{e}(t) = \begin{bmatrix} e_d(t) \\ e_q(t) \end{bmatrix}.$$

With the sampling time h, the model (6) can be discretized as:

$$\begin{cases} \mathbf{x}(k+1) = \mathbf{A}\mathbf{x}(k) + \mathbf{B}\mathbf{u}(k) + \mathbf{D}\mathbf{e}(k) \\ \mathbf{y}(k) = \mathbf{C}\mathbf{x}(k) \end{cases} \tag{7}$$

where $\mathbf{A} = \mathbf{I}_{2\times2} + h\mathbf{A}_c$, $\mathbf{B} = h\mathbf{B}_c$, $\mathbf{D} = \mathbf{D}_c$, and $\mathbf{I}_{2\times2}$ is identity matrix.

Uncertainty Model and Controller Design

The uncertainty model of the system and controller design steps are presented in this section. The uncertainty of the GCI system can be considered a variation of the inductance and resistance values of the *L*-filter with an assumed range. Suppose that the inductance and resistance in each phase are equal but lie within the range below:

$$L_{\min} \le L \le L_{\max} \tag{8}$$

$$R_{\min} \le R \le R_{\max}. \tag{9}$$

Denote the pair of system dynamic $(\mathbf{A}_i, \mathbf{B}_i)$ where (i = 1,2,3,4) in (7) correspond to the four possible combinations of the extreme value of L and R:

$$\begin{aligned}
(\mathbf{A}_1,\mathbf{B}_1) &= \left(\mathbf{I}_{2\times2} + h\begin{bmatrix} -\frac{R_{\max}}{L_{\max}} & \omega \\ -\omega & -\frac{R_{\max}}{L_{\max}} \end{bmatrix}, h\begin{bmatrix} \frac{1}{L_{\max}} & 0 \\ 0 & \frac{1}{L_{\max}} \end{bmatrix}\right),\\
(\mathbf{A}_2,\mathbf{B}_2) &= \left(\mathbf{I}_{2\times2} + h\begin{bmatrix} -\frac{R_{\min}}{L_{\min}} & \omega \\ -\omega & -\frac{R_{\min}}{L_{\min}} \end{bmatrix}, h\begin{bmatrix} \frac{1}{L_{\min}} & 0 \\ 0 & \frac{1}{L_{\min}} \end{bmatrix}\right),\\
(\mathbf{A}_3,\mathbf{B}_3) &= \left(\mathbf{I}_{2\times2} + h\begin{bmatrix} -\frac{R_{\min}}{L_{\max}} & \omega \\ -\omega & -\frac{R_{\min}}{L_{\max}} \end{bmatrix}, h\begin{bmatrix} \frac{1}{L_{\max}} & 0 \\ 0 & \frac{1}{L_{\max}} \end{bmatrix}\right),\\
(\mathbf{A}_4,\mathbf{B}_4) &= \left(\mathbf{I}_{2\times2} + h\begin{bmatrix} -\frac{R_{\max}}{L_{\min}} & \omega \\ -\omega & -\frac{R_{\max}}{L_{\min}} \end{bmatrix}, h\begin{bmatrix} \frac{1}{L_{\min}} & 0 \\ 0 & \frac{1}{L_{\min}} \end{bmatrix}\right).
\end{aligned} \tag{10}$$

To eliminate the steady state offset error which is regulating the system output $\mathbf{y}(k)$ to the reference $\mathbf{i}_{ref}$ which is

$$\mathbf{x}_0 = \mathbf{A}\mathbf{x}_0 + \mathbf{B}\mathbf{u}_0 \tag{11}$$

$$\mathbf{i}_{ref} = \mathbf{C}\mathbf{x}_0. \tag{12}$$

where $\mathbf{x}_0$ represents steady state and $\mathbf{u}_0$ denotes steady state input.

The control law [31] can be defined for (7) as follow

$$\begin{cases} \mathbf{n}(k) = \mathbf{n}(k-1) + \left(\mathbf{y}(k-1) - \mathbf{i}_{ref}\right) \\ \mathbf{u}(k) = \mathbf{K}_x\mathbf{x}(k) + \mathbf{K}_i\mathbf{n}(k) \end{cases}. \tag{13}$$

The control law (13) can be rewritten as [32]:

$$\mathbf{u}(k) - \mathbf{u}(k-1) = \mathbf{K}_x\left(\mathbf{x}(k) - \mathbf{x}(k-1)\right) + \mathbf{K}_i(\mathbf{y}(k-1) - \mathbf{i}_{ref}). \tag{14}$$

Based on (7), (11), (12) and (14), the closed-loop dynamic can be obtained as

$$\mathbf{z}(k+1) = \mathbf{A}_u\mathbf{z}(k) + \mathbf{B}_u(\mathbf{u}(k) - \mathbf{u}_0) \tag{15}$$

where

$$\mathbf{u}(k) - \mathbf{u}_0 = \mathbf{K}\mathbf{z}(k),\ \mathbf{z}(k) := \begin{bmatrix} \mathbf{x}(k) - \mathbf{x}_0 \\ \mathbf{n}(k) - \mathbf{n}(\infty) \end{bmatrix},\ \mathbf{K} := \begin{bmatrix} \mathbf{K}_x & \mathbf{K}_i \end{bmatrix},$$

$$\mathbf{A}_u := \begin{bmatrix} \mathbf{A} & 0_{2\times2} \\ \mathbf{C} & \mathbf{I}_{2\times2} \end{bmatrix}, \text{ and } \mathbf{B}_u := \begin{bmatrix} \mathbf{B} \\ 0_{2\times2} \end{bmatrix}.$$

The origin of the closed-loop dynamic

$$\mathbf{z}(k+1) = (\mathbf{A}_u + \mathbf{B}_u\mathbf{K})\mathbf{z}(k) \tag{16}$$

is asymptotically stable if there exist positive definite matrices $\mathbf{Q} = \mathbf{Q}^T > 0$ and $\mathbf{Y}$ such that

$$\begin{bmatrix} \mathbf{Q} & \left(\mathbf{A}_{ui}\mathbf{Q} + \mathbf{B}_{ui}\mathbf{Y}\right)^T \\ \mathbf{A}_{ui}\mathbf{Q} + \mathbf{B}_{ui}\mathbf{Y} & \mathbf{Q} \end{bmatrix} > 0 \ (i = 1,2,3,4) \tag{17}$$

where $\mathbf{A}_{ui} := \begin{bmatrix} \mathbf{A}_i & 0_{2\times2} \\ \mathbf{C} & \mathbf{I}_{2\times2} \end{bmatrix}$, $\mathbf{B}_{ui} := \begin{bmatrix} \mathbf{B}_i \\ 0_{2\times2} \end{bmatrix}$.

The condition (17) also holds for some $\mathbf{Q}_0 > 0$ ($\mathbf{Q}_0 < \mathbf{Q}$) which

$$\begin{bmatrix} \mathbf{Q}_0 & \left(\mathbf{A}_{ui}\mathbf{Q} + \mathbf{B}_{ui}\mathbf{Y}\right)^T \\ \mathbf{A}_{ui}\mathbf{Q} + \mathbf{B}_{ui}\mathbf{Y} & \mathbf{Q} \end{bmatrix} > 0 \ (i = 1,2,3,4). \tag{18}$$

The stabilizing gain can be computed as

$$\mathbf{K} = \mathbf{Y}\mathbf{Q}_o^{-1} \tag{19}$$

where

$$\mathbf{Q} < \gamma\mathbf{Q}_0 \quad (0 < \gamma < 1). \tag{20}$$

It is expected that the minimal γ yield faster convergence rate of the augmented state $\mathbf{z}(k)$ to the origin. Thus, an optimization problem is needed to be solved to obtain stabilizing gain $\mathbf{K}$, and the generalized eigenvalue problem [33] can be expressed as

Minimize γ subject to (18) and (20)

$$\begin{matrix} \mathbf{Q},\mathbf{Q}_0 > 0 \\ \gamma > 0, \mathbf{Y} \end{matrix} \tag{21}$$

The YALMIP [34] toolbox in MATLAB can be effectively used to tackle this optimization problem.

Reference States Computation

In this section, a simple current reference computation is discussed using current, voltage and power relationship. Output power delivery is regulated by amount of current flow and direction, then the relation can be given in *dq*-synchronous frame as

$$\begin{cases} P = \frac{3}{2}\left(e_d i_d + e_q i_q\right) \\ Q = \frac{3}{2}\left(e_d i_d - e_q i_d\right) \end{cases} \tag{22}$$

where P and Q are active and reactive power, respectively. To obtain the current equation (22) can be rewritten as

$$\begin{cases} i_d = \frac{2}{3M}(e_d P - e_q Q) \\ i_q = \frac{2}{3M}(e_q P + e_d Q) \end{cases} \tag{23}$$

where $M = e_d^2 + e_q^2$, the reference current can be expressed as

$$\begin{cases} i_d^{ref} = \frac{2}{3M}\left(e_d P_{ref} - e_q Q_{ref}\right) \\ i_q^{ref} = \frac{2}{3M}\left(e_q P_{ref} + e_d Q_{ref}\right) \end{cases}. \tag{24}$$

Reactive power needs to be reduced if the power factor is to remain at unity. As a result, the equation (24) can be rewritten to

$$\begin{cases} i_d^{ref} = \frac{2e_d P_{ref}}{3M} \\ i_q^{ref} = \frac{2e_q P_{ref}}{3M} \end{cases}. \tag{25}$$

It is preferable to include reactive power in the controller design since, in some applications, it needs to be regulated to a specific level. Therefore, the reference current that corresponds to (24) can then be written as

$$\mathbf{i}_{ref} = \begin{bmatrix} i_d^{ref} \\ i_q^{ref} \end{bmatrix} = \frac{2}{3M}\begin{bmatrix} e_d & -e_q \\ e_q & e_d \end{bmatrix}\begin{bmatrix} P_{ref} \\ Q_{ref} \end{bmatrix}. \tag{26}$$

The simplified control block diagram is shown in Figure 2.

Simulation Studies

The simulation of the proposed control system is implemented using MATLAB and PSIM tools. Robust optimal control gain **K** is determined by solving optimizing problems in equations (21) and (19) using the LMI toolbox (YALMIP) in MATLAB as offline. Besides that, the computed control gain is applied to the mathematical model of the control system which is written in C language. Then this model is embedded in the dll function block in PSIM and the control algorithm is implemented in the simulation model which is built in PSIM. For the implementation of the model, the nominal system parameters given in Table 1 are used.

Table 1. Proposed system parameters

Parameters	Symbols	Value
Grid phase voltage	$\mathbf{e}_{abc}$	230V (rms)
Nominal filter resistance	R_x	0.1Ω
Nominal filter inductance	L_x	3mH
Sampling period	h	100μs

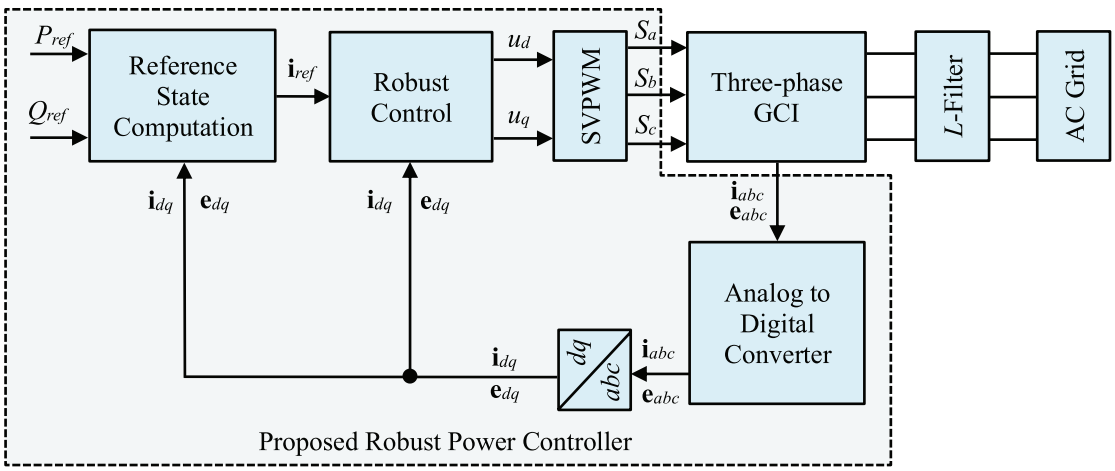

Figure 2. The general block diagram of the proposed system.

Simulation Using Different Parameters And Uncertainty Ranges

The maximum and minimum values of the parameters given in (8) and (9) could be defined using an uncertainty range norm, as in (27) and (28) to express the effects of the various uncertainty range (28). Different values of the inductance and resistor are calculated for different η, as shown in Table 2. Afterward, the transient behavior of the grid current is validated as in Figure 3 using these different values.

$$L_x / \eta \le L_x \le \eta L_x, \tag{27}$$

$$R_x / \eta \le R_x \le \eta R_x \qquad (0 < \eta < 1). \tag{28}$$

It can be seen that the use of narrow uncertainty range results in faster convergence. In contrast, employing a wider range yield a bit of sluggish performance of the output current. Moreover, it is important to evaluate the stability of the nominal and uncertain system considering the eigenvalues of the closed-loop system. Figure 4 and Figure 5 show the eigenvalues of the nominal and uncertain systems, respectively. The stability of the uncertain system is

Table 2. Upper and lower range of the parameters correspond to uncertainty range η

Uncertainty Range	η=1.1	η=1.3	η=1.5	η=1.8	η=2.0
Rmin [Ω]	0.090	0.077	0.067	0.056	0.050
Rmax [Ω]	0.110	0.130	0.150	0.18	0.200
Lmin [mH]	2.730	2.310	2.000	1.667	1.500
Lmax [mH]	3.300	3.900	4.500	5.400	6.000

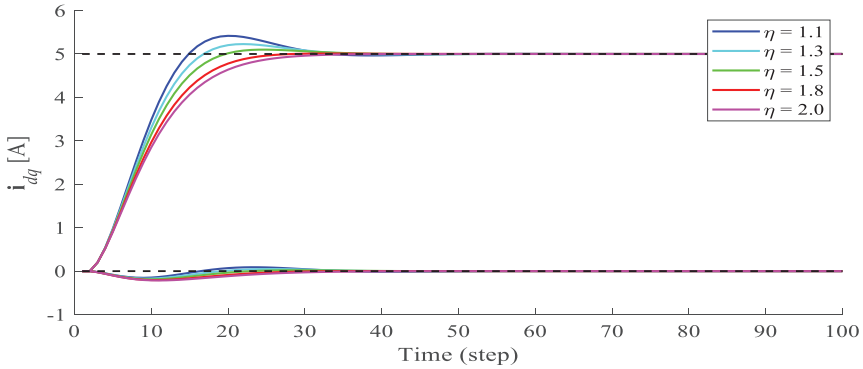

Figure 3. Transient performances of grid currents in *dq*-frame using different uncertainty range.

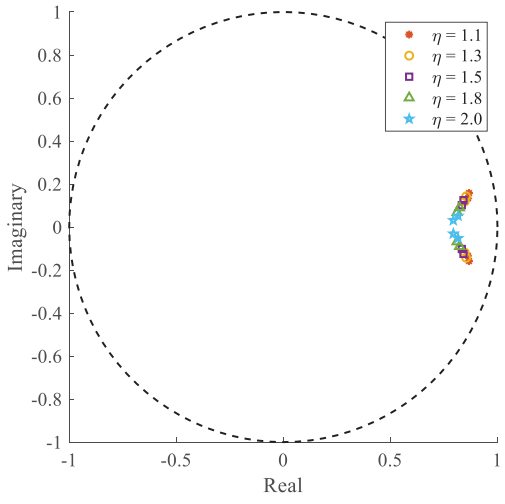

Figure 4. Closed loop eigen values using nominal model with different uncertainty. range

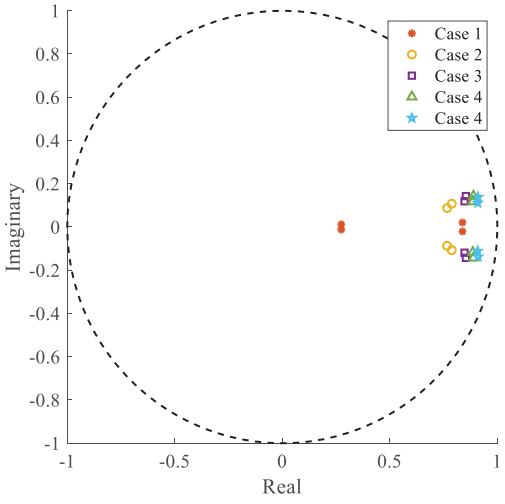

Figure 5. Closed loop eigen values using uncertainty range η = 1.8 with different. parameter iteration cases.

Table 3. Parameters variation cases using the same gain η=1.8

Parameters	Case 1	Case 2	Case 3	Case 4	Case 5
R [Ω]	0.010	0.050	0.100	0.150	0.200
L [mH]	1.000	2.000	3.000	4.000	5.000

evaluated for η = 1.8 under the five cases given in Table 3. The parameter variation is tried to be shown by changing the resistance and inductance values for η = 1.8 which is chosen for the simulations as a design parameter. Thus, it is shown that the uncertain system is stable within the given limits. It is clear that the stability of the closed loop system is unaffected by variations in inductance and filter values within the defined range as seen in Figure 5.

Simulation Using Stepping Power Reference and Grid Voltage Variation

To track the phase angle from the grid side voltage, it is important to use the phase-locked loop (PLL) [35]. After the determination of the grid-phase angle, three-phase signals, i.e., voltage and current can be transformed to the dq-signals with DC quantities since the control system is designed in dq reference frame. In Figure 6, the phase A voltage of grid (a) is shown along with the phase angle (b) obtained by PLL.

The steady-state performance of the proposed control system is evaluated for reference tracking performance of the active and reactive power for η = 1.8 as seen in Figure 7c. The active power reference P_{ref} is set to zero at t = 0 to t = 0.05 s, then it is increased to 2000 W at t = 0.05 s and to 4000 W at t = 0.125 s. On the other hand, the reactive power reference is set to zero for the whole simulation process to maintain a unity power factor. It is important to note that in some applications the reactive power is not required to be set to zero, therefore the reference state can be computed using equation (24) with the given amount of active and reactive power. Figures 7a and 7b show the grid voltages and currents respectively. The results show that the proposed method yields faster transient response and good reference tracking under uncertainties.

To further check the robustness of this proposed method, the reference current tracking performance is evaluated under the grid voltage variation. Figure 8a shows the change in the grid voltage between time intervals 0 s to 0.1 s, 0.1 s to 0.2 s, 0.2 s to 0.3 s, and 0.3 s to 0.4 sec respectively. The current reference is given as 20A from t=0sec to 0.4sec. It is seen that the output current in the *abc*-frame (Figure 8b) and *dq*-frame (Figure 8c) follow the reference under the voltage change.

Comparative Result with Conventional PI Control

To compare the performance of the proposed method with the classical controller, a conventional PI power controller is designed based on the structure represented in

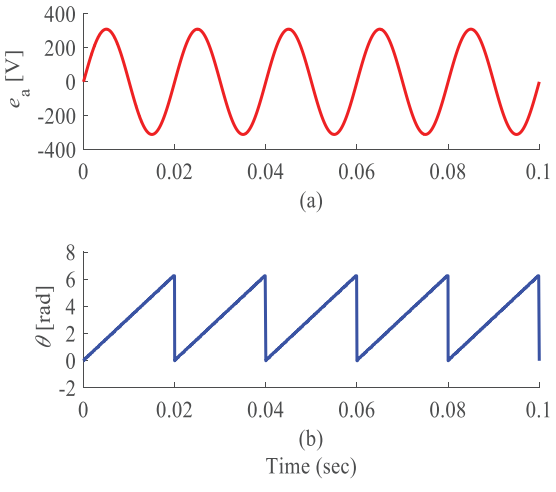

Figure 6. PLL's performance of grid angle tracking, (a) phase-a grid voltage, (b) phase angle.

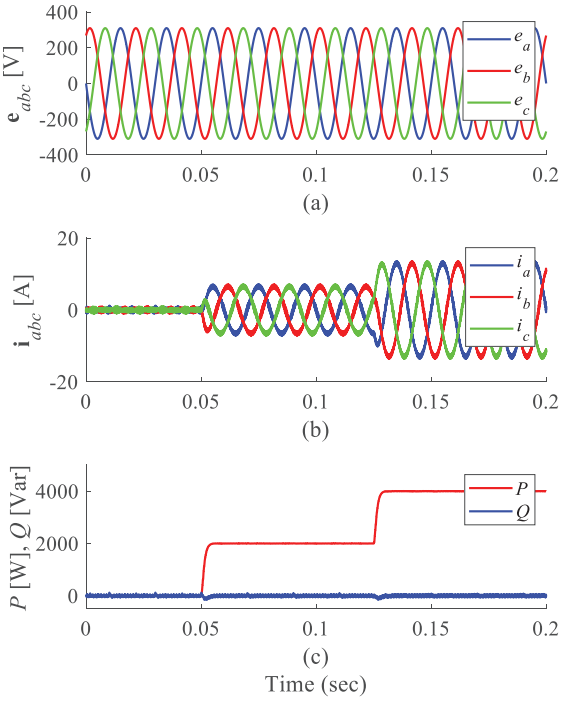

Figure 7. Inverter under variable power reference, (a) grid voltage eabc, (b) grid current iabc, (c) active and reactive power.

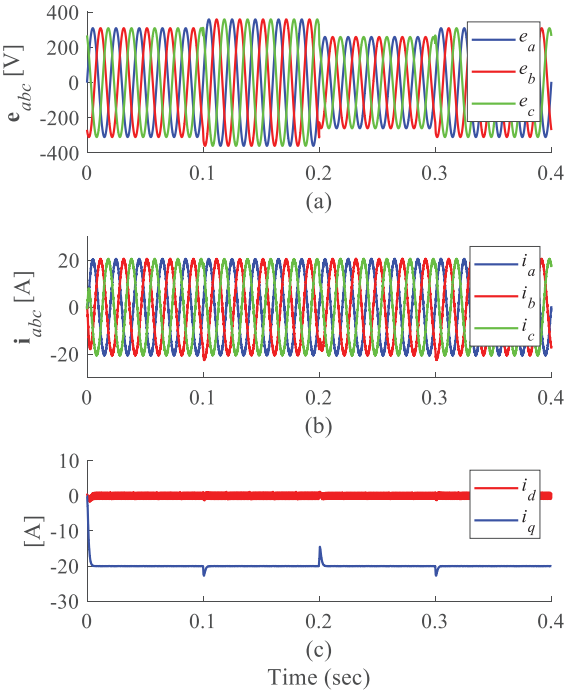

Figure 8. Inverter under variable grid voltage, (a) grid volage with variation between time, (b) grid current, (c) active and reactive power.

Figure 9. The PI gains are obtained by trial and error and their values are shown in table 4. In order to ensure a fair comparison, the performance was adjusted manually until

Table 4. PI gain parameters

Gain	Kp	Ki
id gain	50	1600
iq gain	50	1600

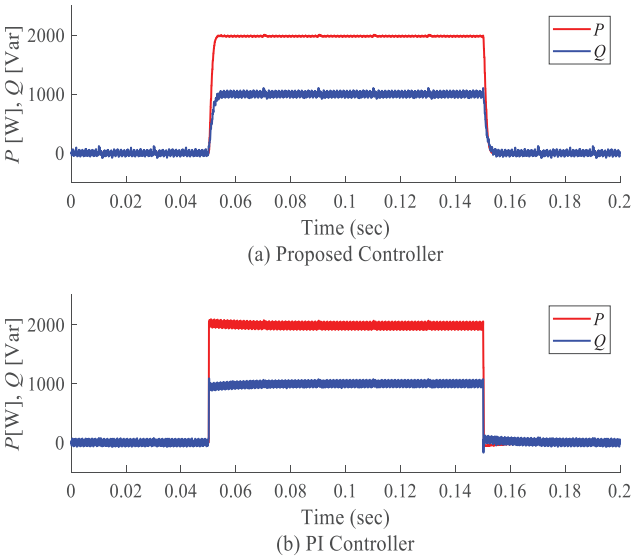

Figure 10. Output active and reactive power using (a) proposed robust control and (b) conventional PI control.

the transient response exhibited comparable levels of performance. Furthermore, the evaluation of the performance of these two controllers does not consider the transient power output as the PI controller is not an optimal control strategy. It is important to acknowledge that the utilization of integral time-weighted absolute error (ITAE) or alternative tuning approaches may yield better results for the PI controller. However, given that the primary emphasis of this study does not lie in this aspect, the straightforward approach of trial and error is employed instead. The PI controller also uses reference state computation to compute the current reference for the desired active and reactive power.

The results of both controllers are shown in Figure 10, where (a) are the result of the proposed method and (b) is the result of PI control. At the steady-state, performance of these two controllers is identical. The proposed method does,

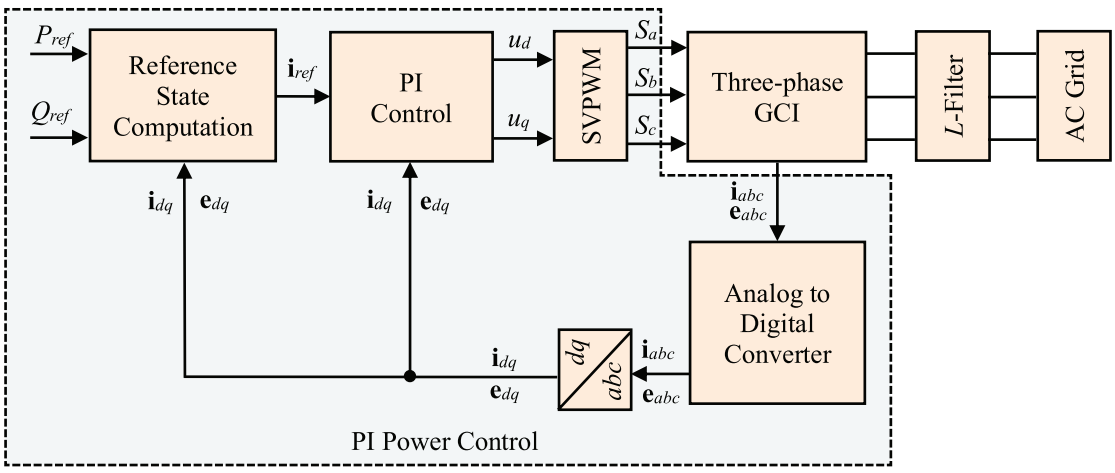

Figure 9. Conventional PI control structure of the three-phase GCI.

however, perform better overall since the active power side has less ripple. The power ripple ΔP exhibited by the proposed control approach is around 20 W, in contrast to the 150 W power ripple seen in the PI control method when operating at a power reference of 2 kW. In summary, the robust control method being proposed shows a reduction in ripple of 86.66% compared to the PI control approach. Furthermore, by relying on only the computed gain, the proposed method requires less work to get the best performance.

CONCLUSION

This proposed study aims to provide well-regulated power delivery from the DC source to the grid through a systematic control design for a three-phase grid-connected inverter. Previous research, such as MPC, required high computational power and precise modeling in order to obtain offset-free performance. Achieving optimal performance in the case of PI control poses a persistent challenge in terms of gain tuning. This proposed control strategy effectively addresses the aforementioned issues through the utilization of systematic control design, incorporating integral action to mitigate the presence of offset error. Moreover, LMI optimizes the stabilizing gain of this controller to minimize the convergence time. Based on the simulation results of the proposed method, it can be said that the output power is effectively transferred to the grid by using a current reference that is calculated based on the active and reactive power that is wanted. This proposed robust control method shows a reduction in ripple of 86.66% compared to the PI control approach.

ACKNOWLEDGMENTS

This work is supported by National Polytechnic Institute of Cambodia.

AUTHORSHIP CONTRIBUTIONS

Authors equally contributed to this work.

DATA AVAILABILITY STATEMENT

The authors confirm that the data that supports the findings of this study are available within the article. Raw data that support the finding of this study are available from the corresponding author, upon reasonable request.

CONFLICT OF INTEREST

The author declared no potential conflicts of interest with respect to the research, authorship, and/or publication of this article.

ETHICS

There are no ethical issues with the publication of this manuscript.

REFERENCES

[1] Al-Dori O, Şakar B, Dönük A. Comprehensive analysis of losses and leakage reactance of distribution transformers. Arab J Sci Eng 2022;47:14163–14171. [CrossRef]

[2] Dönük A, Al-Dori O. Performance and harmonic analysis of a three-phase induction motor with various coil pitch configurations. Yüzüncü Yıl Üniversitesi Fen Bilimleri Enstitüsü Dergisi 2023;28:38–47. [CrossRef]

[3] Al-Dori O, Şakar B, Dönük A. Optimal design and performance analysis of three-phase distribution transformer with variable loading. Electric Power Compon Syst 2022;50:458–468. [CrossRef]

[4] Huang L, Wu C, Zhou D, Blaabjerg F. Impact of grid strength and impedance characteristics on the maximum power transfer capability of grid-connected inverters. Appl Sci 2021;11:4288. [CrossRef]

[5] Etxegarai A, Eguia P, Torres E, Iturregi A, Valverde V. Review of grid connection requirements for generation assets in weak power grids. Renew Sustain Energy Rev 2015;41:1501–1514. [CrossRef]

[6] Collins L, Ward JK. Real and reactive power control of distributed PV inverters for overvoltage prevention and increased renewable generation hosting capacity. Renew Energy. 2015;81:464–471. [CrossRef]

[7] Chen J, Yang F, Han QL. Model-free predictive H∞ control for grid-connected solar power generation systems. IEEE Trans Contr Syst Technol 2014;22:2039–2047. [CrossRef]

[8] Liao H, Zhang X, Ma Z. Robust dichotomy solution-based model predictive control for the grid-connected inverters with disturbance observer. Trans Electr Mach Syst 2021;5:81–89. [CrossRef]

[9] Song Z, Chen W, Xia C. Predictive direct power control for three-phase grid-connected converters without sector information and voltage vector selection. IEEE Trans Power Electron 2014;29:5518–5531. [CrossRef]

[10] Judewicz MG, Gonzalez SA, Fischer JR, Martinez JF, Carrica DO. Inverter-side current control of grid-connected voltage source inverters with LCL filter based on generalized predictive control. IEEE J Emerg Sel Topics Power Electron 2018;6:1732–1743. [CrossRef]

[11] Kim Y, Tran TV, Kim KH. LMI-based model predictive current control for an LCL-filtered grid-connected inverter under unexpected grid and system uncertainties. Electronics 2022;11:731. [CrossRef]

[12] Qin G, Chen Q, Zhang L. Finite control set model predictive control based on three-phase four-leg grid-connected inverters. 2020 35th Youth Academic Annual Conference of Chinese Association of Automation (YAC), Zhanjiang, China: IEEE; 2020. p. 680–684. [CrossRef]

[13] Moreno JC, Espi Huerta JM, Gil RG, Gonzalez SA. A robust predictive current control for three-phase grid-connected inverters. IEEE Trans Ind Electron 2009;56:1993–2004. [CrossRef]

[14] Espi Huerta JM, Castello-Moreno J, Fischer JR, Garcia-Gil R. A synchronous reference frame robust predictive current control for three-phase grid-connected inverters. IEEE Trans Ind Electron 2010;57:954–962. [CrossRef]

[15] Ma L, Zheng TQ. Synchronous PI control for three-phase grid-connected photovoltaic inverter. 2010 Chinese Control and Decision Conference, Xuzhou, China: IEEE; 2010. p. 2302–2307. [CrossRef]

[16] Alqatamin M, Latham J, Smith ZT, Grainger BM, McIntyre ML. Current control of a three-phase, grid-connected inverter in the presence of unknown grid parameters without a phase-locked loop. IEEE J Emerg Sel Topics Power Electron 2021;9:3127–3136. [CrossRef]

[17] Mirhosseini M, Pou J, Agelidis VG. Current improvement of a grid-connected photovoltaic system under unbalanced voltage conditions. 2013 IEEE ECCE Asia Downunder, Melbourne, Australia: IEEE; 2013. p. 66–72. [CrossRef]

[18] Liu J, Wu W, Chung HS-H, Blaabjerg F. Disturbance observer-based adaptive current control with self-learning ability to improve the grid-injected current for LCL-filtered grid-connected inverter. IEEE Access 2019;7:105376–105390. [CrossRef]

[19] Yoon SJ, Lai NB, Kim KH. A systematic controller design for a grid-connected inverter with LCL filter using a discrete-time integral state feedback control and state observer. Energies 2018;11:437. [CrossRef]

[20] Pena JCU, Sampaio LP, Canesin CA. A LMI-based control of a three-phase voltage source inverter capable to operate in islanded and grid connected modes. 2015 IEEE 13th Brazilian Power Electronics Conference and 1st Southern Power Electronics Conference (COBEP/SPEC), Fortaleza: IEEE; 2015. p. 1–6. [CrossRef]

[21] Lim JS, Park C, Han J, Lee YI. Robust tracking control of a three-phase DC-AC inverter for UPS applications. IEEE Trans Ind Electron 2014;61:4142–151. [CrossRef]

[22] Barden AT, Alves Pereira LF. Robust control design of multiple resonant controllers applied to three-phase UPS inverter under unbalanced and nonlinear loads. IECON 2015 - 41st Annual Conference of the IEEE Industrial Electronics Society, Yokohama: IEEE; 2015. p. 001483–001488. [CrossRef]

[23] Danayiyen Y, Lee K, Choi M, Lee YI. Model predictive control of uninterruptible power supply with robust disturbance observer. Energies 2019;12:2871. [CrossRef]

[24] Kim SK, Park CR, Yoon TW, Lee YI. Disturbance-observer-based model predictive control for output voltage regulation of three-phase inverter for uninterruptible-power-supply applications. Eur J Control 2015;23:71–83. [CrossRef]

[25] Huy V, Tang H, Soth P, Yay S, Sovan K, Choeung C. Three-phase inverter using robust tracking control based interpolation. 2023 Third International Symposium on Instrumentation, Control, Artificial Intelligence, and Robotics (ICA-SYMP), Bangkok, Thailand: IEEE; 2023. p. 91–95. [CrossRef]

[26] Saggin F, Coutinho D, Heldwein ML. Parallel operation of single-phase voltage source inverters: Modeling and control based on LMI constraints. IECON 2016 - 42nd Annual Conference of the IEEE Industrial Electronics Society, Florence, Italy: IEEE; 2016. p. 270–275. [CrossRef]

[27] Choeung C, Kry ML, Lee YI. Robust tracking control of a three-phase bidirectional charger for electric vehicle. J Adv Transp 2022;2022:1–12. [CrossRef]

[28] Fitri I, Kim JS, Song H. A robust suboptimal current control of an interlink converter for a hybrid AC/DC microgrid. Energies 2018;11:1382. [CrossRef]

[29] Choeung C, Tang H, Soth P, Keo S, Leang P, Cheng H, et al. Linear matrix inequality-based optimal state feedback control of a three-phase L-filtered grid-connected inverter. 2023 Third International Symposium on Instrumentation, Control, Artificial Intelligence, and Robotics (ICA-SYMP), Bangkok, Thailand: IEEE; 2023. p. 135–139. [CrossRef]

[30] Soth P, Tang H, So B, San S, Cheng H, Choeung C, et al. Robust dual-current control of a three-phase grid-tied inverter under unbalanced grid voltage using LMI approach. 2023 International Electrical Engineering Congress (iEECON), Krabi, Thailand: IEEE; 2023. p. 6–11. [CrossRef]

[31] Choeung C, Kry ML, Lee YI. Robust tracking control of a three-phase charger under unbalanced grid conditions. Energies 2018;11:3389. [CrossRef]

[32] Açıkmeşe AB, Corless M. Robust output tracking for uncertain/nonlinear systems subject to almost constant disturbances. Automatica 2002;38:1919–1926. [CrossRef]

[33] Boyd SP, editor. Linear matrix inequalities in system and control theory. Philadelphia: Society for Industrial and Applied Mathematics; 1994. [CrossRef]

[34] Lofberg J. YALMIP: a toolbox for modeling and optimization in MATLAB. 2004 IEEE International Conference on Robotics and Automation (IEEE Cat. No.04CH37508), Taipei, Taiwan: IEEE; 2004. p. 284–289.

[35] Tang H, In S, Soth P, Soeng S, Cheng H, Huy V, et al. Design of a robust control for a single-phase AC-DC converter using LMI technique. 2023 International Electrical Engineering Congress (iEECON), Krabi, Thailand: IEEE; 2023. p. 1–5. [CrossRef]